

¹ Provenance of Life: Chemical Autonomous Agents Surviving
² Through Associative Learning

³ Stuart Bartlett ^{1,2}, and David Louapre ^{3,4}

¹ Division of Geological and Planetary Sciences,
California Institute of Technology,
Pasadena, CA 91125, United States

² Earth-Life Science Institute,
Tokyo Institute of Technology, Tokyo 152-8550, Japan

³ Ubisoft Entertainment Research & Development, 94160 Saint-Mandé, France

⁴ Science Étonnante, 75014 Paris, France

⁴ February 11, 2021

⁵ **Abstract**

⁶ Reaction-diffusion spots can learn!

⁷ Ever since the outspoken Nobel Laureate Ilya Prigogine introduced the concept, dissipative structures
⁸ and their underlying phenomenology have beguiled, entranced and split opinions of researchers from
⁹ a range of disciplines [1, 2]. The approximate definition of a dissipative structure is a coherent and
¹⁰ discernible dynamical pattern that is maintained by external disequilibria over a finite timescale. The
¹¹ structure exists at a higher phenomenological or descriptive level to its microscopic constituents, and
¹² can thus be considered ‘emergent’ [3, 4, 5, 6, 7]. Being driven by external disequilibria is of course a
¹³ necessary condition, since this makes the system dissipative.

¹⁴ The most frequently cited examples of dissipative structures are fluid convection cells [8, 9, 10, 11,
¹⁵ 12], hurricanes [13], dynamic surfactant structures such as micelles, vesicles and droplets [14, 15, 16,
¹⁶ 17, 18, 19], stars and galaxies [20], black holes [21], and biological organisms [22, 23, 24]. In the
¹⁷ fields of Artificial Life and the Origins of Life, dissipative structures are a key focus area, serving as
¹⁸ metaphors for simple forms of life and providing clues to the non-life to life transition [25, 26, 27, 28,
¹⁹ 29]. Numerous experiments and simulations in this field have illustrated the emergence of subsets of
²⁰ life’s properties in non-living systems. For example, various oil droplet systems have been shown to
²¹ readily exhibit chemotaxis, in which the motion of the droplets is powered through the consumption
²² of a fuel compound, and the droplets’ motion naturally follows gradients in the concentration of that
²³ fuel compound [15, 16, 28, 30, 31, 32, 33, 34]. Self-replication is a common phenomenon in reaction-
²⁴ diffusion systems (RDSs) [24, 27, 35, 36, 37, 38, 39, 40, 41] and vesicle-based structures, also known
²⁵ as protocells [42, 43, 44, 45, 46, 47, 48, 49, 50, 51]. Non-living or artificial dissipative structures
²⁶ have also exhibited ecological behaviour including competition [35, 37, 52], homeostasis [53] and
²⁷ symbiosis [36, 54]. Artificial cell studies generally follow the model of autopoiesis [55]¹, in that
²⁸ they seek integrated cellular structures comprising a boundary or membrane, a metabolic system for

¹which is closely related to the ‘chemoton’ concept [56] and the container-metabolism-program doctrine [57]

29 converting precursor ‘food’ molecules into the components of the cell, and an information system that
30 is normally analogous to a genetic apparatus [46, 47, 51, 58, 59, 60, 61].

31 While pursuing a parsimonious, ‘straight-shot’ from prebiotic physics and chemistry to biology is a
32 logical starting point in seeking the origins of life, given the often bizarre twists and turns that life
33 and its evolutionary path have taken [62, 63, 64], it is also possible that the earliest forms of life
34 were not simplified versions of extant life, but rather different in composition and organization. A
35 natural question thus arises: what are the conserved quantities that we expect extant life, early life,
36 and even extraterrestrial life, to exhibit? While ‘definitions of life’ abound, and much previous work
37 was inspired by the autopoiesis and chemoton doctrines, a definition has recently been introduced
38 that combines traditional and modern ideas from thermodynamics, biology, information theory and
39 cognitive science [65]. This ‘four pillared’ definition suggests that a living system must exhibit all of
40 the following properties: 1) Dissipation (the system must be exposed to one or more thermodynamic
41 disequilibrium or free energy source), 2) Autocatalysis (the system must exhibit or have the capacity
42 to exhibit exponential growth of a representative size metric such as population under ideal condi-
43 tions), 3) Homeostasis (the system must possess regulatory or negative feedback mechanisms that can
44 mitigate external or internal perturbations), 4) Learning (the system must have the ability to sense,
45 store, process and exploit information).

46 While various model protocell systems have primitive genetic components, and simpler artificial
47 chemical systems exhibit self-replication, chemotaxis, and homeostasis, emergent learning in sim-
48 ple artificial systems has remained an elusive goal. Chemical computing itself is a large discipline
49 that includes the incredible achievements of DNA computing [66, 67, 68, 69, 70], computing using
50 the Belousov-Zhabotinsky reaction [71, 72, 73, 74, 75, 76, 77, 78, 79] and more general approaches
51 that exploit the computational universality and associative abilities of chemical reaction networks
52 [80, 81, 82, 83, 84, 85, 86, 87, 88, 89, 90, 91, 92]. Chemical computation has also been exploited
53 for the control of agent-like entities such as simple robots [93], but such robots are not emergent and
54 hence their analysis is primarily a heuristic tool for the engineering of swarm intelligence (as opposed
55 to understanding the origins of life).

56 Despite the great strides described above, the problem of the emergence of a self-organised entity
57 that satisfies a minimal definition of life including a basic learning ability, is still very much open.
58 Complex protocells that are scaled-down versions of extant life provide extensive but fundamentally
59 limited guidance to the origins of life, since they require a relatively high threshold of *a priori* design.
60 In the present work, we explored a minimal complexity, emergent system that exhibits all the features
61 of minimal life definitions, including the four pillars of ‘lyfe’ [65], autopoiesis [55], and the ability
62 to perform associative learning. The ability to grow autocatalytically, mitigate external perturbations,
63 and carry out learning all emerge spontaneously and are not explicitly written into the equations of
64 motion of the system.

65 We have thus reduced the lower bound on the required simplicity of an emergent, autonomous agent
66 capable of learning. Our approach can be extended to much larger learning networks. Given the vast
67 space of prebiotic reaction networks, there is more than enough available computational potential at
68 the origins of life. The key challenge is understanding the conditions in which learning becomes the
69 most stable dynamical pattern in a system (the learning has to feed back positively on the stability of
70 the pattern).

71 Our approach is based upon the soliton-like spatially organised instabilities that form in non-linear
72 chemical systems, collectively known as reaction diffusion structures (RDΣs) [24, 27, 35, 36, 37, 38,

73 39, 41, 54, 94, 95, 96, 97, 98, 99, 100, 101, 102, 103, 104]. The systematic understanding of RDSs
74 traces all the way back to Turing, who introduced their founding principles alongside the foundations
75 of morphogenesis, which became one of the pioneering triumphs of mathematical biology [105]. The
76 RDS used in the present work is commonly known as the Gray-Scott model (GSM) [38, 39, 41, 102,
77 106, 107], which is itself an elaboration of the Selkov model of glycolysis [108]. The GSM is a
78 simple 2-dimensional RDS that has been shown to exhibit life-like emergent properties. It involves
79 two chemical species, denoted A and B, interacting through a simple auto-catalytic reaction $A + 2B \rightarrow 3B$. Along with an appropriate supply mechanism for A and removal mechanism for B, this
80 reaction produces a variety of patterns, including self-replicating spots, able to progressively colonise
81 a region of space [41]. In addition, previous work has shown that adding the thermal dimension to this
82 system (original versions were isothermal) reveals even more layers of emergent phenomena including
83 competition (between RD Σ s and convection cells) [37], and thermal homeostasis through symbiotic
84 thermal regulation [36].

85
86 Although the GSM exhibits life-like properties, it lacks an essential feature of life which is learning.
87 Broadly speaking, *learning* can be defined as the ability of a system to record information about its
88 environment, and process that information to modulate its behavior. It is believed that learning is an
89 essential pillar of life [109], providing a sensitivity to the environment that can improve the survival
90 probability of the living system². Although learning is sometimes viewed as specific to organisms
91 having a nervous system, a large and rapidly expanding list of non-neural learning mechanisms illus-
92 trate its biological ubiquity [110], and it is hypothesized that learning may have played a role in life's
93 origins [111, 112, 113, 114, 115]. Among the different learning mechanisms, associative learning is
94 particularly relevant in that regard. It can be defined as the ability for a system to detect and record
95 *correlated* features about its environment. Let us illustrate how this could play a role in the resilience
96 and adaptability of a living system.

97 Consider a system within an environment where a chemical species I is periodically delivered, and
98 results in the formation of a toxin T . If the synthesis of T from I is sufficiently slow, the delivery of
99 I acts as a stimulus that will signal the occurrence of T ahead of time. Assuming the system is able
100 to synthesise an antidote O , it might be more efficient to do it as soon as stimulus I is detected, since
101 it would provide an anticipating defense against the toxin (if a gazelle can see a cheetah coming from
102 a distance, it has a better chance of surviving an attack than if the cheetah pounces from behind). For
103 instance in the simplest case, the synthesis of O would be directly catalysed by I . Let us denote this
104 simple network by \mathcal{N}_D (for "Direct").

105 Now suppose that the production of T from I also depends on slowly varying environmental factors
106 (such as temperature, pH, or the concentration of other species), so that the presence of I does not
107 systematically result in the synthesis of T . There might be some environmental conditions \mathcal{E}_1 where
108 a delivery of I is actually followed by the occurrence of T , and some other environmental conditions
109 \mathcal{E}_0 where this not the case. If the environment were to change from \mathcal{E}_1 to \mathcal{E}_0 , the direct network \mathcal{N}_D
110 would still produce the antidote O every time I is delivered, even if it is not followed by the toxin
111 T . As the production of the antidote O could be a costly mechanism, or the antidote itself might be a
112 mild toxin, this unnecessary production would end up damaging the system.

113 To avoid this, a more efficient network should have the ability to detect and record whether, in its
114 current environment, I is actually followed by T or not. It would then adapt if the environmental

²this includes fields such as cognitive science, 4E cognition (embodied, embedded, enactive, and extended), perception-action cycles, measurement-feedback protocols, etc.

	Environment \mathcal{E}_1 $I \Rightarrow T$	Environment \mathcal{E}_0 $I \Rightarrow \emptyset$
No network	Death from toxin	No toxin No antidote
Direct network \mathcal{N}_D	Toxin neutralized by antidote	Unnecessary production of antidote
Associative network \mathcal{N}_A	Toxin neutralized by antidote	No toxin No antidote

Figure 1: Expected behaviour of different antidote production mechanisms in environment \mathcal{E}_1 where stimulus I is followed by T , and \mathcal{E}_0 where stimulus I is present but no toxin T is produced.

115 conditions were to change, for instance in the case of a transition from \mathcal{E}_1 to \mathcal{E}_0 or vice-versa. Fulfilling
 116 this requirement is an associative learning task, since the system is required to detect whether I is
 117 followed by T , record that information and react accordingly, while being able to update its behavior
 118 if the link between I and T disappears. Let us denote by \mathcal{N}_A a chemical network that would perform
 119 such associative learning.

120 Figure 1 summarizes the expected behavior of those two networks \mathcal{N}_D and \mathcal{N}_A in the two environments \mathcal{E}_1 and \mathcal{E}_0 . Our goal in this paper is to show that such an associative learning network \mathcal{N}_A can
 121 be realized using a very simple chemical network. As described above, chemical computing is already
 122 a well-developed field, and approaches to chemical learning have been suggested [85, 86, 87, 88, 91].
 123 The approach used in the present work was inspired by the learning networks of [116]. Using search
 124 methods inspired by evolutionary processes, they were able to find abstract chemical networks able to
 125 solve learning tasks (such as basic association, and the AB-BA task, where a system has to learn the
 126 order in which two stimuli occur, and adapt its output accordingly). However, their search involved a
 127 very large parameter space (searched using an evolutionary algorithm), and it was difficult to interpret
 128 what were the essential features of those networks that made them relevant for the learning tasks, and
 129 how to choose the values of the different parameters involved. Furthermore, the learning networks
 130 were not embodied within emergent chemical structures.
 131

132 The aim of the present work is twofold: 1) to explore minimally complex reaction systems that clearly
 133 confer associative learning abilities, 2) to see whether such networks can be embedded within emerg-
 134 ent, spatially distinct, self-organised chemical structures. Such phenomena would serve as an impor-
 135 tant guide to the conditions in which the basic properties of life can emerge. Crucially, this emergence
 136 occurs in the complete absence of large molecules, peptides, nucleic acids, biochemical reactions,
 137 metabolic cycles or membrane structures, and hence lowers the bar on the necessary conditions for
 138 chemical, autonomous, cognitive agents.

139 In the first part of this work, we present minimal chemical networks that efficiently solve the learning
 140 tasks described above, when placed in a well-stirred (0-dimensional) environment. In the second part
 141 of the paper, we show how to extend those results to a 2-dimensional case, where the learning network
 142 is coupled to a self-replicating spot system from the GSM. This provides a realisation of a dissipative
 143 structure able to replicate and adapt to its environment using associative learning, a feat which, as far

144 as we are aware, has not been achieved before.

145 1 Learning chemical networks in well-stirred, 0-dimensional Systems

146 1.1 Model and network design

147 Let us first describe how to model the environment (that defines the learning task to be solved) and
148 the two networks \mathcal{N}_D ('direct network') and \mathcal{N}_A ('associative network'), that we designed.

149 Our model involves 6 chemical species (denoted I , P , T , S_I , L and O) interacting through a small
150 set of chemical reactions. Only stimulus I is externally delivered, and all species are progressively
151 removed through exponential decay (with a specific characteristic time τ_i for each species i). Below
152 we describe the reactions constituting the environment dynamics, the direct network \mathcal{N}_D and the
153 associative learning network \mathcal{N}_A .

154 Environment: Species I is periodically delivered as boluses of unit concentration, with a temporal
155 period \mathcal{T} (we use $\mathcal{T} = 100$). I degrades exponentially and we choose a short characteristic time
156 ($\tau_I = 0.05\mathcal{T} = 5$), so that I quickly disappears after each bolus. Stimulus I will serve as a signaling
157 cue for the later occurrence of toxin T , so we assume I catalyzes the production of a certain precursor
158 P (from another background compound that is omitted for simplicity), that is in turn converted into
159 T :



160 We choose reaction constants $k_P = 1$ and $k_T = 0.05$; the rate constant k_P will control the final
161 amount of toxin produced after each bolus, while the small value of k_T ensures the peak of T will
162 occur after the bolus of I . The characteristic decay time of T is set at $\tau_T = 0.2\mathcal{T} = 20$, so it
163 essentially disappears between each delivery.

164 Those settings define environmental condition \mathcal{E}_1 , where T is produced after I is delivered. Environment
165 \mathcal{E}_0 is simply achieved by setting k_P to zero, so that no toxin is produced. The dynamics of these
166 environments are illustrated in Figure 2 (top panel).

167 Finally, we assume that the toxin T can be degraded by the antidote O , via a chemical reaction where
168 they both react to produce inert waste



169 where $k_A = 0.1$. To enforce the fact that O should be produced in a timely manner, we use a moderate
170 characteristic decay time of $\tau_O = \mathcal{T} = 100$.

171 Direct network: The simple, 'instantaneous' response of network \mathcal{N}_D only involves one reaction in
172 which output antidote O production is directly catalysed by the presence of I :



173 where k_D can be tuned to vary the strength of the response.

174 Associative network: The associative learning network \mathcal{N}_A involves two additional species: S_I acting
175 as a short term memory, and L acting as a long term memory. Production of species S_I is catalyzed

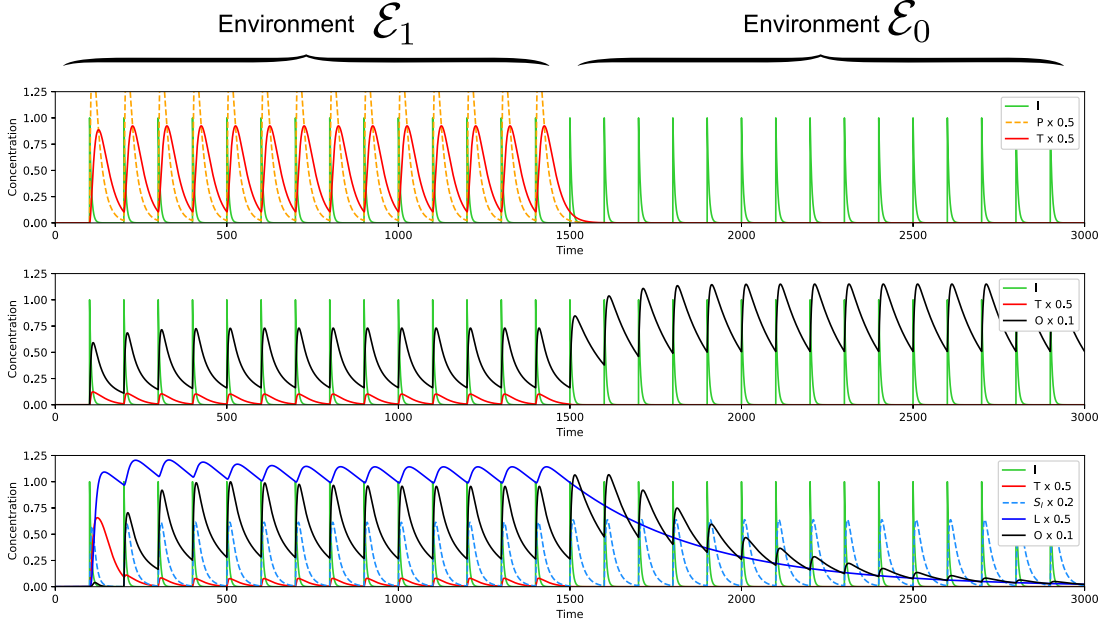


Figure 2: Concentration time series for the two environments \mathcal{E}_1 and \mathcal{E}_0 . Top panel: Environment dynamics without network. Reaction constant k_P is set to zero after 1500 steps, switching from environment \mathcal{E}_1 to \mathcal{E}_0 . Middle panel: Dynamics of the direct network \mathcal{N}_D with $k_D = 1.66$. Bottom panel: Dynamics of the associative learning network \mathcal{N}_A when $k_L = 0.051$.

176 by the presence of I :



177 To act as short-term memory, its decay characteristic time should be longer than that of the bolus, and
 178 of the order of the expected separation time between the bolus and the peak of T . Hence we choose
 179 $\tau_{S_I} = 0.2\mathcal{T} = 20$.

180 Species L must be produced from S_I in the presence of T , hence recording the fact that a bolus of I
 181 has actually been followed by the occurrence of T :



182 To serve as a long term memory, the characteristic decay time of L should be of the order of a few times
 183 the period \mathcal{T} , reflecting the rate at which the system will learn and adapt to a varying environment.
 184 We choose $\tau_L = 4\mathcal{T} = 400$.

185 Finally for this network, production of species O must be catalyzed by the long term memory com-
 186 pound L in the presence of stimulus I (the relevant supply compound for O is omitted):



187 In this description of the associative network \mathcal{N}_A , three reaction rates k_S , k_L and k_O have been
 188 so far left unspecified, and can in principle be tuned to vary the dynamics and the strength of the
 189 response. However, from the three reactions involved in the network, it can be seen that the amount

190 of O produced essentially only depends on the product $k_S k_L k_O$. Hence we choose to set $k_S = 1$ and
 191 $k_O = 1$, and use only k_L as a free parameter when performing sensitivity analyses.

192 Simulation: We simulate the dynamics of the networks and the environment with a set of coupled
 193 ordinary differential equations. If $\{C_i\}_{i=1..N}$ represents the set of N chemical species, subject to R
 194 reactions, the time evolution of concentration ψ_{C_i} is given by

$$\frac{\partial \psi_{C_i}}{\partial t} = - \sum_{r=1}^R k_r [\alpha'_{ri} - \alpha^*_{ri}] \prod_{j=1}^N \psi_{C_j}^{\alpha'_{rj}},$$

195 where α'_{ri} is the left hand side stoichiometric coefficient for reaction r and chemical species i (the
 196 number of molecules of species i entering as reactants into reaction r), and α^*_{ri} is the right hand side
 197 stoichiometric coefficient for reaction r and chemical species i (the number of molecules of species i
 198 leaving as products from reaction r). Here we have ignored the role of temperature, and k_r denotes the
 199 reaction constant of reaction r . Reactions are simulated only in the forward direction, and possible
 200 reverse reactions are considered as extra, separate reactions from their forward counterparts. The
 201 exponential decay of each species is included as a reaction.

202 We simulated the networks coupled to the environment over 3000 time steps, starting with zero con-
 203 centrations for all species. We use explicit time forward Euler integration ($dt = 0.1$). After 1500 time
 204 steps, the value of k_P is turned to zero, simulating a change from \mathcal{E}_1 to \mathcal{E}_0 .

205 Optimal values of k_D (for the direct network \mathcal{N}_D) and k_L (for the associative network \mathcal{N}_A) were
 206 found using line search optimisation. As a cost function, we computed the temporal average of the
 207 concentration of the toxin $\langle \psi_T \rangle$ and of the output $\langle \psi_O \rangle$, and used the weighted sum:

$$\kappa = \langle \psi_T \rangle + \gamma \langle \psi_O \rangle \quad (8)$$

208 with $\gamma = 0.01$. This reflects the fact that the output antidote can be seen as a mild toxin (or a costly
 209 production), and that the elimination of the toxin should result in a trade-off with antidote production.

210 1.2 Results

211 After appropriately tuning the reaction constants, we obtained the results displayed in Figure 2, with
 212 $k_D = 1.66$ for \mathcal{N}_D and $k_L = 0.051$ for \mathcal{N}_A .

213 In environment \mathcal{E}_1 , boluses of I are followed by spikes of T . The direct network \mathcal{N}_D then properly
 214 produces output O to degrade the toxin T . As the output is triggered by I , it is produced slightly before
 215 the toxin would reach its peak, effectively providing an anticipating defense mechanism. However
 216 after switching from \mathcal{E}_1 to \mathcal{E}_0 , the network continues to unnecessarily produce output O , while there
 217 is no more toxin produced.

218 In the case of the associative learning network \mathcal{N}_A , each time I is followed by T , long term memory
 219 L builds up, enabling the anticipated production of output O , which then degrades toxin T . When
 220 the toxin production is switched off in \mathcal{E}_0 , the presence of I is no longer followed by T . Long term
 221 memory L then decreases, progressively turning off the production of O . It thus provides an effective
 222 associative learning mechanism, recording information about its environment, using this information
 223 to react accordingly, while adapting its behavior when the external environment changes.

224 It can be seen that despite the learning mechanism, complete elimination of the toxin does not occur.
 225 This is because the system reaches a dynamic equilibrium through a feedback mechanism. Since

226 the renewal of L is catalyzed by the presence of the toxin T , an excessive production of O would
 227 remove more of the toxin, and hence reduce the renewal of L , which would subsequently decrease
 228 the output. Conversely if the initial output is too low, due to excessive toxin, L keeps increasing with
 229 a concomitant increase in O . At equilibrium, the residual level of toxin provides just the necessary
 230 exposure to renew the long term memory.

231 This feedback mechanism is elegantly demonstrated when the environment slowly oscillates between
 232 \mathcal{E}_1 and \mathcal{E}_0 , as shown in Figure 3. We simply modulated the reaction constant k_P , which governs
 233 the amount of toxin produced. We can see that the exact same network \mathcal{N}_A performs well in such
 234 a task, and learns to adapt to the amount of toxin present. Long term memory variations L closely
 235 track the variation of k_P , showing that the network can effectively learn this environmental parameter
 236 in a continuous fashion. It adapts its behavior while continuously updating its knowledge about the
 237 environment.

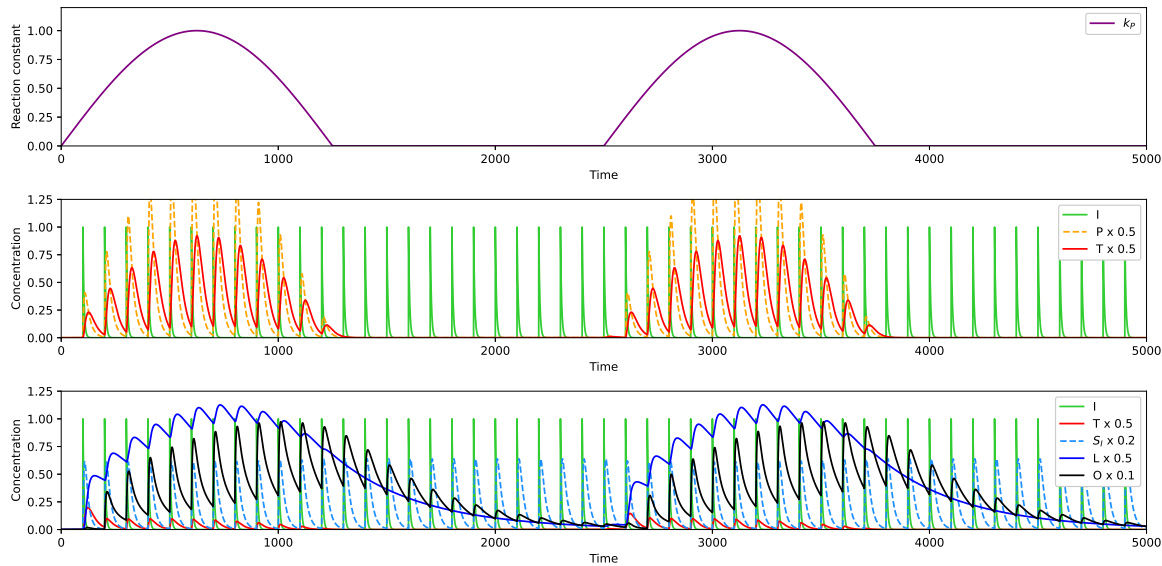


Figure 3: Top: Modulation of k_P , dictating the strength of toxin production from boluses of I . Middle: Dynamics of the environment without any learning network interaction. Bottom: behavior of the associative network \mathcal{N}_A in this varying environment. Network reaction constants are the same as shown previously.

238 Since the network revises its knowledge at every bolus (with a period T), and has a natural response
 239 time τ_L , the evolution of L over time can be seen as the result of a discrete low-pass filter applied to
 240 k_P . This is a natural interpretation since at each bolus, the network samples k_P as the strength of the
 241 association between I and T , and updates the level of L based on this. This is exactly what a discrete
 242 low pass filter does³

³The discrete low-pass filter of a signal x_n is a signal y_n such that $y_{n+1} = (1 - \alpha)y_n + \alpha x_n$. The parameter α governs the learning speed. For a low pass filter (RC) with characteristic time $RC = \tau$ and discrete signal sampled with time step \mathcal{T} , we find $\alpha = \mathcal{T}/(\mathcal{T} + \tau)$.

²⁴³ **2 Learning chemical networks in 2D reaction-diffusion systems**

²⁴⁴ We now consider similar networks, but embed them in a 2D environment, coupled to a Gray-Scott
²⁴⁵ RDS. Hence there is a spatial dependence for the concentration of every species.

²⁴⁶ **2.1 Model description**

²⁴⁷ The model uses a 256×128 grid with a spacing of $dx = 1$, and an isotropic diffusion coefficient for
²⁴⁸ each species. The GSM consists of two chemical species A and B, subject to the chemical reaction
²⁴⁹ $A + 2B \longrightarrow 3B$, along with a decay mechanism for B and a supply mechanism for A [38, 39, 41,
²⁵⁰ 102, 106, 107]. The equations of motion for the concentrations of A and B are as follows:

$$\psi_A = D_A \nabla^2 \psi_A - \psi_A \psi_B^2 + f(1 - \psi_A) \quad (9)$$

$$\psi_B = D_B \nabla^2 \psi_B + \psi_A \psi_B^2 + (f + r)\psi_B \quad (10)$$

²⁵¹ with $D_A = 0.2$, $D_B = 0.1$, $f = 0.03$ and $r = 0.061$, a choice of constants known to give rise to
²⁵² self-replicating spots [41]. With this setting, the spots are distinguished by local excess concentrations
²⁵³ of B (relative to the equilibrium concentration of 0), co-located with local deficits in the concentration
²⁵⁴ of A (relative to the equilibrium concentration of 1). We choose the concentration of B as an order
²⁵⁵ parameter for visual representations.

²⁵⁶ To couple the GSM to the chemical networks described in the previous section, we introduce sev-
²⁵⁷ eral changes. For the direct network \mathcal{N}_D , the production of antidote O in the presence of T is now
²⁵⁸ catalyzed by B , to reflect the fact that it is produced by the spots:



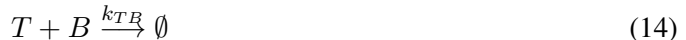
²⁵⁹ Similarly for the associative network \mathcal{N}_A , the production of short-term memory S_I in the presence of
²⁶⁰ I now occurs only in the presence of B:



²⁶¹ and the production of output antidote O in the presence of I and L is also catalyzed by B :



²⁶² To represent the fact that T is a toxic to the RD Σ s, it degrades the B component via the following
²⁶³ reaction:



²⁶⁴ with $k_{TB} = 0.01$. An excess production of O must also be detrimental to the GS Σ s, so we introduce
²⁶⁵ another reaction through which antidote O also causes decay of B :



²⁶⁶ although with a smaller reaction constant $k_{OB} = 0.005$ (simulating the fact that the antidote itself
²⁶⁷ acts as a milder toxin).

²⁶⁸ Bolus delivery: In this spatial system, the delivery mode of the boluses of I is a key consideration. We
²⁶⁹ considered two different cases. In the so-called *uniform* condition, boluses are delivered everywhere in

	D	τ			
I	1.0	100	k_D	0.06	0.025
P	1.0	-	k_S	10	10
T	1.0	50	k_L	2.5e-4	7.5e-5
O	1.0	100	k_O	1	1
S_I	0.2	10	k_A	100	100
L	0.2	10000			

Table 1: Diffusion constants and characteristic decay times for the species involved in the network, along with reaction constants for both the uniform and boundary diffusion conditions.

a homogeneous fashion, as would occur for a 2D system sandwiched between porous plates allowing the transverse diffusion of certain species (this is the way A is supplied and B removed in the GSM). Under this condition, all the GS Σ s come under equivalent attack from the toxin. We use boluses of duration 0.1 and concentration 0.3, with $k_P = 0.05$. The next delivery mode to consider is the *boundary diffusion* condition, in which the boluses are delivered on the boundary of the domain, and infiltrate through diffusion. For this condition, we used boluses of duration 1 and concentration 1, with $k_P = 0.1$. We use $k_T = 0.05$ in both conditions for the synthesis of T from P .

The concentration of A is initialised homogeneously to $\psi_A^{t=0} = 1$. To provide the initial seeds for the development of the GS Σ s, for each grid point $\psi_B^{t=0} = 1$ with a probability of 0.35, and $\Psi_B = 0$ otherwise. To ensure the GS Σ s have time to fully develop before the toxin arrives, the boluses start after 2000 time steps.

The parameters of the reaction network were manually adjusted from the values found for the 0D case. We set $k_S = 10$, $k_O = 1$ and $k_A = 100$, adjusting only k_D for the direct network \mathcal{N}_D , and k_L for the associative learning network \mathcal{N}_A . Simulations were performed using forward Euler integration with $dt = 0.1$. To speed up the core calculations, the simulation was implemented on a GPU using HLSL compute shaders, and Unity3D software for interface and rendering.

To estimate the evolution of the GS Σ s system while being perturbed by T , we computed the spatial average of ψ_B as a function of time. The number of GS Σ s was also counted using a thresholding and flood-fill procedure applied to the order parameter $\psi_B - \psi_A$ (threshold = -0.3).

2.2 Results

For both modes of bolus delivery (uniform or boundary diffusion), we simulated the two networks \mathcal{N}_D and \mathcal{N}_A in the two conditions: environments \mathcal{E}_1 and \mathcal{E}_0 , with and without toxin production associated with stimulus I , respectively. In addition, we ran a control case with an empty network (no antidote production). Results for the uniform and boundary delivery modes are displayed in Figure 4 and Figure 5, respectively. We can draw similar conclusions for both delivery mechanisms.

In the control case (without any antidote production), the GS Σ s get quickly destroyed by the toxin in \mathcal{E}_1 , and remain stable in \mathcal{E}_0 . For the direct network \mathcal{N}_D , antidote O is released in \mathcal{E}_1 , and prevents the destruction of the GS Σ s. However in \mathcal{E}_0 , the unnecessary production and accumulation of the antidote progressively intoxicates the system, as can be seen from the declining concentration of B and number of spots. However, in the case of the associative learning network \mathcal{N}_A , the defense mechanism is properly activated only when necessary, allowing production of O only in the \mathcal{E}_1 environment. In this condition from the count of spots and the average concentration of B (bottom left of Figure 4 and

302 Figure 5), it is clear that initially the GS Σ s get damaged by the toxin, until the progressive build-up of
303 the long term memory triggers the appropriate response and prevents further destruction. The GS Σ s
304 then replicate autocatalytically and re-invade the space they had lost (see Figure 6 for snapshots of
305 their spatial evolution).

306 **References**

- 307 [1] D. Kondepudi and I. Prigogine. *Modern Thermodynamics: From Heat Engines to Dissipative*
308 *Structures*. Wiley, 2014.
- 309 [2] Ilya Prigogine. Time, structure, and fluctuations. *Science*, 201(4358):777–785, 1978.
- 310 [3] Philip W Anderson et al. More is different. *Science*, 177(4047):393–396, 1972.
- 311 [4] Jeffrey Goldstein. Emergence as a construct: History and issues. *Emergence*, 1(1):49–72,
312 1999.
- 313 [5] Erik P Hoel, Larissa Albantakis, and Giulio Tononi. Quantifying causal emergence shows that
314 macro can beat micro. *Proceedings of the National Academy of Sciences*, 110(49):19790–
315 19795, 2013.
- 316 [6] J.H. Holland. *Emergence: From Chaos to Order*. Popular science / Oxford University Press.
317 Oxford University Press, 2000.
- 318 [7] Steen Rasmussen, Nils A Baas, Bernd Mayer, Martin Nilsson, and Michael W Olesen. Ansatz
319 for dynamical hierarchies. *Artificial life*, 7(4):329–353, 2001.
- 320 [8] Guenter Ahlers, Siegfried Grossmann, and Detlef Lohse. Heat transfer and large scale dynamics
321 in turbulent rayleigh-bénard convection. *Reviews of modern physics*, 81(2):503, 2009.
- 322 [9] Stuart Bartlett and Seth Bullock. Natural convection of a two-dimensional boussinesq fluid
323 does not maximize entropy production. *Physical Review E*, 90(2):023014, 2014.
- 324 [10] Stuart Bartlett and Nathaniel Virgo. Maximum entropy production is not a steady state attractor
325 for 2d fluid convection. *Entropy*, 18(12):431, 2016.
- 326 [11] Paul Manneville. *Rayleigh-Bénard Convection: Thirty Years of Experimental, Theoretical, and*
327 *Modeling Work*, pages 41–65. Springer New York, New York, NY, 2006.
- 328 [12] W Pesch. Complex spatiotemporal convection patterns. *Chaos: An Interdisciplinary Journal*
329 *of Nonlinear Science*, 6(3):348–357, 1996.
- 330 [13] Kerry A Emanuel. The maximum intensity of hurricanes. *Journal of the Atmospheric Sciences*,
331 45(7):1143–1155, 1988.
- 332 [14] Pascale Angelica Bachmann, Pier Luigi Luisi, and Jacques Lang. Autocatalytic self-replicating
333 micelles as models for prebiotic structures. *Nature*, 357(6373):57, 1992.
- 334 [15] Martin M Hanczyc. Metabolism and motility in prebiotic structures. *Philosophical Transactions*
335 *of the Royal Society of London B: Biological Sciences*, 366(1580):2885–2893, 2011.

- 336 [16] Martin M Hanczyc, Taro Toyota, Takashi Ikegami, Norman Packard, and Tadashi Sugawara.
337 Fatty acid chemistry at the oil- water interface: self-propelled oil droplets. *Journal of the*
338 *American Chemical Society*, 129(30):9386–9391, 2007.
- 339 [17] Bernd Mayer, Gottfried Köhler, and Steen Rasmussen. Simulation and dynamics of entropy-
340 driven, molecular self-assembly processes. *Physical Review E*, 55(4):4489, 1997.
- 341 [18] Daniel Segré, Dafna Ben-Eli, David W Deamer, and Doron Lancet. The lipid world. *Origins*
342 *of Life and Evolution of the Biosphere*, 31(1-2):119–145, 2001.
- 343 [19] Ting F Zhu and Jack W Szostak. Coupled growth and division of model protocell membranes.
344 *Journal of the American Chemical Society*, 131(15):5705–5713, 2009.
- 345 [20] Toshiya Nozakura and Satoru Ikeuchi. Formation of dissipative structures in galaxies. *The*
346 *Astrophysical Journal*, 279:40–52, 1984.
- 347 [21] A. Curir. Rotating black holes as dissipative spin-thermodynamical systems. *General Relativity*
348 *and Gravitation*, 13(5):417–423, May 1981.
- 349 [22] Dilip Kondepudi, Bruce Kay, and James Dixon. Dissipative structures, machines, and organ-
350 isms: A perspective. *Chaos: An Interdisciplinary Journal of Nonlinear Science*, 27(10):104607,
351 2017.
- 352 [23] Charles H Lineweaver and Chas A Egan. Life, gravity and the second law of thermodynamics.
353 *Physics of Life Reviews*, 5(4):225–242, 2008.
- 354 [24] Nathaniel D Virgo. *Thermodynamics and the structure of living systems*. PhD thesis, University
355 of Sussex Brighton, 2011.
- 356 [25] Brian J Cafferty, Albert SY Wong, Sergey N Semenov, Lee Belding, Samira Gmür, Wilhelm TS
357 Huck, and George M Whitesides. Robustness, entrainment, and hybridization in dissipa-
358 tive molecular networks, and the origin of life. *Journal of the American Chemical Society*,
359 141(20):8289–8295, 2019.
- 360 [26] Matthew Egbert, Yan Kolezhitskiy, and Nathaniel Virgo. Steering the growth of adaptive self-
361 preserving dissipative structures. In *Artificial Life Conference Proceedings*, pages 255–262.
362 MIT Press, 2019.
- 363 [27] Tom Froese, Nathaniel Virgo, and Takashi Ikegami. Motility at the origin of life: Its character-
364 ization and a model. *Artificial life*, 20(1):55–76, 2014.
- 365 [28] Martin M Hanczyc. Metabolism and motility in prebiotic structures. *Philosophical Transactions*
366 *of the Royal Society B: Biological Sciences*, 366(1580):2885–2893, 2011.
- 367 [29] Doron Lancet, Raphael Zidovetzki, and Omer Markovitch. Systems protobiology: origin of life
368 in lipid catalytic networks. *Journal of The Royal Society Interface*, 15(144):20180159, 2018.
- 369 [30] Jitka Čejková, Matej Novák, František Štěpánek, and Martin M Hanczyc. Dynamics of chemo-
370 tactic droplets in salt concentration gradients. *Langmuir*, 30(40):11937–11944, 2014.
- 371 [31] Jitka Čejková, Silvia Holler, To Quyen Nguyenová, Christian Kerrigan, František Štěpánek,
372 and Martin M Hanczyc. Chemotaxis and chemokinesis of living and non-living objects. In
373 *Advances in unconventional computing*, pages 245–260. Springer, 2017.

- 374 [32] Jitka Čejková, Taisuke Banno, Martin M Hanczyc, and František Štěpánek. Droplets as liquid
375 robots. *Artificial life*, 23(4):528–549, 2017.
- 376 [33] Martin M Hanczyc, Shelly M Fujikawa, and Jack W Szostak. Experimental models of primitive
377 cellular compartments: encapsulation, growth, and division. *Science*, 302(5645):618–622,
378 2003.
- 379 [34] Silvia Holler and Martin Michael Hanczyc. Droplet based synthetic biology: chemotaxis and
380 interface with biology. In *Artificial Life Conference Proceedings*, pages 650–651. MIT Press,
381 2019.
- 382 [35] Stuart Bartlett. *Why is life? An assessment of the thermodynamic properties of dissipative,
383 pattern-forming systems*. PhD thesis, University of Southampton, 2014.
- 384 [36] Stuart Bartlett and Seth Bullock. A precarious existence: Thermal homeostasis of simple dis-
385 sipative structures. *Proceedings of the Artificial Life Conference 2016*, pages 608–615, 2016.
- 386 [37] Stuart Bartlett and Seth Bullock. Emergence of competition between different dissipative struc-
387 tures for the same free energy source. In *Artificial Life Conference Proceedings 13*, pages
388 415–422. MIT Press, 2015.
- 389 [38] Kyoung-Jin Lee, William D McCormick, John E Pearson, and Harry L Swinney. Experimental
390 observation of self-replicating spots in a reaction–diffusion system. *Nature*, 369(6477):215,
391 1994.
- 392 [39] Kyoung J Lee and Harry L Swinney. Lamellar structures and self-replicating spots in a reaction-
393 diffusion system. *Physical Review E*, 51(3):1899, 1995.
- 394 [40] Felipe Lesmes, David Hochberg, Federico Morán, and Juan Pérez-Mercader. Noise-controlled
395 self-replicating patterns. *Physical review letters*, 91(23):238301, 2003.
- 396 [41] John E Pearson. Complex patterns in a simple system. *Science*, 261(5118):189–192, 1993.
- 397 [42] Irene A Chen, Richard W Roberts, and Jack W Szostak. The emergence of competition between
398 model protocells. *Science*, 305(5689):1474–1476, 2004.
- 399 [43] Martin M Hanczyc and Jack W Szostak. Replicating vesicles as models of primitive cell growth
400 and division. *Current opinion in chemical biology*, 8(6):660–664, 2004.
- 401 [44] Tony Z Jia, Kuhan Chandru, Yayoi Hongo, Rehana Afrin, Tomohiro Usui, Kunihiro Myojo,
402 and H James Cleaves. Membraneless polyester microdroplets as primordial compartments at
403 the origins of life. *Proceedings of the National Academy of Sciences*, 116(32):15830–15835,
404 2019.
- 405 [45] Sean F Jordan, Hanadi Ramm, Ivan N Zheludev, Andrew M Hartley, Amandine Maréchal,
406 and Nick Lane. Promotion of protocell self-assembly from mixed amphiphiles at the origin of
407 life. *Nature ecology & evolution*, 3(12):1705–1714, 2019.
- 408 [46] Gerald F Joyce and Jack W Szostak. Protocells and rna self-replication. *Cold Spring Harbor
409 Perspectives in Biology*, 10(9):a034801, 2018.
- 410 [47] Stephen Mann. Systems of creation: the emergence of life from nonliving matter. *Accounts of
411 chemical research*, 45(12):2131–2141, 2012.

- 412 [48] Naoaki Ono. Computational studies on conditions of the emergence of autopoietic protocells.
413 *BioSystems*, 81(3):223–233, 2005.
- 414 [49] Steen Rasmussen, Adi Constantinescu, and Carsten Svaneborg. Generating minimal living
415 systems from non-living materials and increasing their evolutionary abilities. *Philosophical*
416 *Transactions of the Royal Society B: Biological Sciences*, 371(1701):20150440, 2016.
- 417 [50] Ben Shirt-Ediss, Ricard V Solé, and Kepa Ruiz-Mirazo. Emergent chemical behavior in
418 variable-volume protocells. *Life*, 5(1):181–211, 2015.
- 419 [51] Ricard V Solé, Andreea Munteanu, Carlos Rodriguez-Caso, and Javier Macía. Synthetic pro-
420 tocell biology: from reproduction to computation. *Philosophical Transactions of the Royal*
421 *Society B: Biological Sciences*, 362(1486):1727–1739, 2007.
- 422 [52] Katarzyna Adamala and Jack W Szostak. Competition between model protocells driven by an
423 encapsulated catalyst. *Nature chemistry*, 5(6):495, 2013.
- 424 [53] Aaron E Engelhart, Katarzyna P Adamala, and Jack W Szostak. A simple physical mechanism
425 enables homeostasis in primitive cells. *Nature chemistry*, 8(5):448–453, 2016.
- 426 [54] Tom Froese, Takashi Ikegami, and Nathaniel Virgo. The behavior-based hypercycle: From
427 parasitic reaction to symbiotic behavior. *Artificial Life*, 13:457–464, 2012.
- 428 [55] Humberto R Maturana and Francisco J Varela. *Autopoiesis and cognition: The realization of*
429 *the living*, volume 42. Springer Science & Business Media, 2012.
- 430 [56] Tibor Gánti. Organization of chemical reactions into dividing and metabolizing units: the
431 chemotons. *BioSystems*, 7(1):15–21, 1975.
- 432 [57] Steen Rasmussen, Mark A Bedau, John S McCaskill, and Normann H Packaed. A roadmap
433 to protocells. In *Protocells: Bridging Nonliving ans Living Matter*, pages 71–100. MIT Press,
434 2008.
- 435 [58] Alex Joesaar, Shuo Yang, Bas Bögels, Ardjan van der Linden, Pascal Pieters, BVVS Pavan
436 Kumar, Neil Dalchau, Andrew Phillips, Stephen Mann, and Tom FA de Greef. Dna-based
437 communication in populations of synthetic protocells. *Nature nanotechnology*, 14(4):369–378,
438 2019.
- 439 [59] Kensuke Kurihara, Yusaku Okura, Muneyuki Matsuo, Taro Toyota, Kentaro Suzuki, and
440 Tadashi Sugawara. A recursive vesicle-based model protocell with a primitive model cell cycle.
441 *Nature communications*, 6(1):1–7, 2015.
- 442 [60] Mei Li, Xin Huang, TY Dora Tang, and Stephen Mann. Synthetic cellularity based on non-
443 lipid micro-compartments and protocell models. *Current opinion in chemical biology*, 22:1–11,
444 2014.
- 445 [61] Yan Qiao, Mei Li, Richard Booth, and Stephen Mann. Predatory behaviour in synthetic proto-
446 cell communities. *Nature chemistry*, 9(2):110–119, 2017.
- 447 [62] Sean B Carroll. Chance and necessity: the evolution of morphological complexity and diversity.
448 *Nature*, 409(6823):1102–1109, 2001.

- 449 [63] Sean B Carroll. *A Series of Fortunate Events: Chance and the Making of the Planet, Life, and*
450 *You*. Princeton University Press, 2020.
- 451 [64] Stephen Jay Gould and Elisabeth S Vrba. Exaptation-a missing term in the science of form.
452 *Paleobiology*, pages 4–15, 1982.
- 453 [65] Stuart Bartlett and Michael L. Wong. Defining lyfe in the universe: From three privileged
454 functions to four pillars. *Life*, 10(4):42, Apr 2020.
- 455 [66] Roy Bar-Ziv, Tsvi Tlusty, and Albert Libchaber. Protein–dna computation by stochastic assem-
456 bly cascade. *Proceedings of the National Academy of Sciences*, 99(18):11589–11592, 2002.
- 457 [67] Yaakov Benenson. Biomolecular computing systems: principles, progress and potential. *Nature*
458 *Reviews Genetics*, 13(7):455–468, 2012.
- 459 [68] Johann Elbaz, Oleg Lioubashevski, Fuan Wang, Françoise Remacle, Raphael D Levine,
460 and Itamar Willner. Dna computing circuits using libraries of dnazyme subunits. *Nature*
461 *nanotechnology*, 5(6):417–422, 2010.
- 462 [69] Lulu Qian, Erik Winfree, and Jehoshua Bruck. Neural network computation with dna strand
463 displacement cascades. *Nature*, 475(7356):368–372, 2011.
- 464 [70] Ehud Shapiro and Yaakov Benenson. Bringing dna computers to life. *Scientific American*,
465 294(5):44–51, 2006.
- 466 [71] Andrew Adamatzky and Benjamin De Lacy Costello. Experimental logical gates in a reaction-
467 diffusion medium: The xor gate and beyond. *Physical Review E*, 66(4):046112, 2002.
- 468 [72] Marta Dueñas-Díez and Juan Pérez-Mercader. In-vitro reconfigurability of native chemical
469 automata, the inclusiveness of their hierarchy and their thermodynamics. *Scientific reports*,
470 10(1):1–12, 2020.
- 471 [73] J Gorecki, K Gizynski, J Guzowski, JN Gorecka, P Garstecki, G Gruenert, and P Dittrich.
472 Chemical computing with reaction–diffusion processes. *Philosophical Transactions of the*
473 *Royal Society A: Mathematical, Physical and Engineering Sciences*, 373(2046):20140219,
474 2015.
- 475 [74] W Hohmann, M Kraus, and FW Schneider. Learning and recognition in excitable chemical
476 reactor networks. *The Journal of Physical Chemistry A*, 102(18):3103–3111, 1998.
- 477 [75] Julian Holley, Ishrat Jahan, Ben De Lacy Costello, Larry Bull, and Andrew Adamatzky. Log-
478 ical and arithmetic circuits in belousov-zhabotinsky encapsulated disks. *Physical Review E*,
479 84(5):056110, 2011.
- 480 [76] Juan Manuel Parrilla-Gutierrez, Abhishek Sharma, Soichiro Tsuda, Geoffrey JT Cooper, Ger-
481 ardo Aragon-Camarasa, Kevin Donkers, and Leroy Cronin. A programmable chemical com-
482 puter with memory and pattern recognition. *Nature communications*, 11(1):1–8, 2020.
- 483 [77] Oliver Steinbock, Petteri Kettunen, and Kenneth Showalter. Chemical wave logic gates. *The*
484 *Journal of Physical Chemistry*, 100(49):18970–18975, 1996.
- 485 [78] Mingzhu Sun and Xin Zhao. Combinational logic circuit based on bz reaction. In *Advances in*
486 *Unconventional Computing*, pages 105–139. Springer, 2017.

- 487 [79] AL Wang, JM Gold, N Tompkins, M Heymann, KI Harrington, and S Fraden. Configurable nor
488 gate arrays from belousov-zhabotinsky micro-droplets. *The European Physical Journal Special*
489 *Topics*, 225(1):211–227, 2016.
- 490 [80] Wolfgang Banzhaf, Peter Dittrich, and Hilmar Rauhe. Emergent computation by catalytic
491 reactions. *Nanotechnology*, 7(4):307, 1996.
- 492 [81] Wolfgang Banzhaf and Lidia Yamamoto. *Artificial chemistries*. MIT Press, 2015.
- 493 [82] Ho-Lin Chen, David Doty, and David Soloveichik. Deterministic function computation with
494 chemical reaction networks. *Natural computing*, 13(4):517–534, 2014.
- 495 [83] Marta Dueñas-Díez and Juan Pérez-Mercader. How chemistry computes: language recognition
496 by non-biochemical chemical automata. from finite automata to turing machines. *Iscience*,
497 19:514–526, 2019.
- 498 [84] Johann Gasteiger and Jure Zupan. Neural networks in chemistry. *Angewandte Chemie*
499 *International Edition in English*, 32(4):503–527, 1993.
- 500 [85] Allen Hjelmfelt, Edward D Weinberger, and John Ross. Chemical implementation of neural
501 networks and turing machines. *Proceedings of the National Academy of Sciences*,
502 88(24):10983–10987, 1991.
- 503 [86] Allen Hjelmfelt and John Ross. Chemical implementation and thermodynamics of collective
504 neural networks. *Proceedings of the National Academy of Sciences*, 89(1):388–391, 1992.
- 505 [87] Allen Hjelmfelt, FW Schneider, and John Ross. Pattern recognition in coupled chemical kinetic
506 systems. *Science*, 260(5106):335–337, 1993.
- 507 [88] A Hjelmfelt and J Ross. Implementation of logic functions and computations by chemical
508 kinetics. *Physica D: Nonlinear Phenomena*, 84(1-2):180–193, 1995.
- 509 [89] Marcelo O Magnasco. Chemical kinetics is turing universal. *Physical Review Letters*,
510 78(6):1190, 1997.
- 511 [90] František Muzika and Igor Schreiber. Control of turing patterns and their usage as sensors,
512 memory arrays, and logic gates. *The Journal of chemical physics*, 139(16):164108, 2013.
- 513 [91] William Poole, Andrés Ortiz-Munoz, Abhishek Behera, Nick S Jones, Thomas E Ouldridge,
514 Erik Winfree, and Manoj Gopalkrishnan. Chemical boltzmann machines. In *International*
515 *Conference on DNA-Based Computers*, pages 210–231. Springer, 2017.
- 516 [92] David Soloveichik, Matthew Cook, Erik Winfree, and Jehoshua Bruck. Computation with finite
517 stochastic chemical reaction networks. *natural computing*, 7(4):615–633, 2008.
- 518 [93] Kyran Dale and Phil Husbands. The evolution of reaction-diffusion controllers for minimally
519 cognitive agents. *Artificial life*, 16(1):1–19, 2010.
- 520 [94] MA Budroni and Anne De Wit. Dissipative structures: From reaction-diffusion to
521 chemo-hydrodynamic patterns. *Chaos: An Interdisciplinary Journal of Nonlinear Science*,
522 27(10):104617, 2017.

- 523 [95] Irving R Epstein. Predicting complex biology with simple chemistry. *Proceedings of the*
524 *National Academy of Sciences*, 103(43):15727–15728, 2006.
- 525 [96] Irving R Epstein and Bing Xu. Reaction–diffusion processes at the nano-and microscales.
526 *Nature nanotechnology*, 11(4):312, 2016.
- 527 [97] P Gray and SK Scott. Sustained oscillations and other exotic patterns of behavior in isothermal
528 reactions. *The Journal of Physical Chemistry*, 89(1):22–32, 1985.
- 529 [98] Peter Gray, Stephen K Scott, and John H Merkin. The brusselator model of oscillatory reactions.
530 relationships between two-variable and four-variable models with rigorous application of
531 mass conservation and detailed balance. *Journal of the Chemical Society, Faraday Transactions*
532 *1: Physical Chemistry in Condensed Phases*, 84(4):993–1011, 1988.
- 533 [99] J Halatek and E Frey. Rethinking pattern formation in reaction–diffusion systems. *Nature*
534 *Physics*, 14(5):507, 2018.
- 535 [100] Maxim Kuznetsov, Andrey Kolobov, and Andrey Polezhaev. Pattern formation in a reaction-
536 diffusion system of fitzhugh-nagumo type before the onset of subcritical turing bifurcation.
537 *Physical Review E*, 95(5):052208, 2017.
- 538 [101] YN Kyrychko, KB Blyuss, SJ Hogan, and E Schöll. Control of spatiotemporal patterns in the
539 gray–scott model. *Chaos: An Interdisciplinary Journal of Nonlinear Science*, 19(4):043126,
540 2009.
- 541 [102] Kyoung J Lee, WD McCormick, Qi Ouyang, and Harry L Swinney. Pattern formation by
542 interacting chemical fronts. *Science*, 261(5118):192–194, 1993.
- 543 [103] Hitoshi Mahara, Kosuke Suzuki, Rumana Akther Jahan, and Tomohiko Yamaguchi. Coexisting
544 stable patterns in a reaction-diffusion system with reversible gray-scott dynamics. *Physical*
545 *Review E*, 78(6):066210, 2008.
- 546 [104] H-G Purwins, HU Bödeker, and AW Liehr. Dissipative solitons in reaction-diffusion systems.
547 In *Dissipative solitons*, pages 267–308. Springer, 2005.
- 548 [105] Alan Mathison Turing. The chemical basis of morphogenesis. *Phil. Trans. R. Soc. Lond. B*,
549 237(641):37–72, 1952.
- 550 [106] P Gray and SK Scott. Sustained oscillations and other exotic patterns of behavior in isothermal
551 reactions. *The Journal of Physical Chemistry*, 89(1):22–32, 1985.
- 552 [107] Peter Gray, Stephen K Scott, and John H Merkin. The brusselator model of oscillatory reactions.
553 relationships between two-variable and four-variable models with rigorous application of
554 mass conservation and detailed balance. *Journal of the Chemical Society, Faraday Transactions*
555 *1: Physical Chemistry in Condensed Phases*, 84(4):993–1011, 1988.
- 556 [108] EE Sel’Kov. Self-oscillations in glycolysis 1. a simple kinetic model. *European Journal of*
557 *Biochemistry*, 4(1):79–86, 1968.
- 558 [109] Keith D Farnsworth, John Nelson, and Carlos Gershenson. Living is information processing:
559 from molecules to global systems. *Acta biotheoretica*, 61(2):203–222, 2013.

- 560 [110] František Baluška and Michael Levin. On having no head: cognition throughout biological
561 systems. *Frontiers in psychology*, 7:902, 2016.
- 562 [111] Stuart J Bartlett and Patrick Beckett. Probing complexity: Thermodynamics and computational
563 mechanics approaches to origins studies. *Interface focus*, 9(6):20190058, 2019.
- 564 [112] Tom Froese, Jorge I Campos, Kosuke Fujishima, Daisuke Kiga, and Nathaniel Virgo. Horizontal
565 transfer of code fragments between protocells can explain the origins of the genetic code
566 without vertical descent. *Scientific reports*, 8(1):1–10, 2018.
- 567 [113] Denis Michel. Life is a self-organizing machine driven by the informational cycle of brillouin.
568 *Origins of Life and Evolution of Biospheres*, 43(2):137–150, 2013.
- 569 [114] Sara Imari Walker and Paul CW Davies. The algorithmic origins of life. *Journal of the Royal*
570 *Society Interface*, 10(79):20120869, 2013.
- 571 [115] Sara Imari Walker. Top-down causation and the rise of information in the emergence of life.
572 *Information*, 5(3):424–439, 2014.
- 573 [116] Simon McGregor, Vera Vasas, Phil Husbands, and Chrisantha Fernando. Evolution of associative
574 learning in chemical networks. *PLoS Comput Biol*, 8(11):e1002739, 2012.

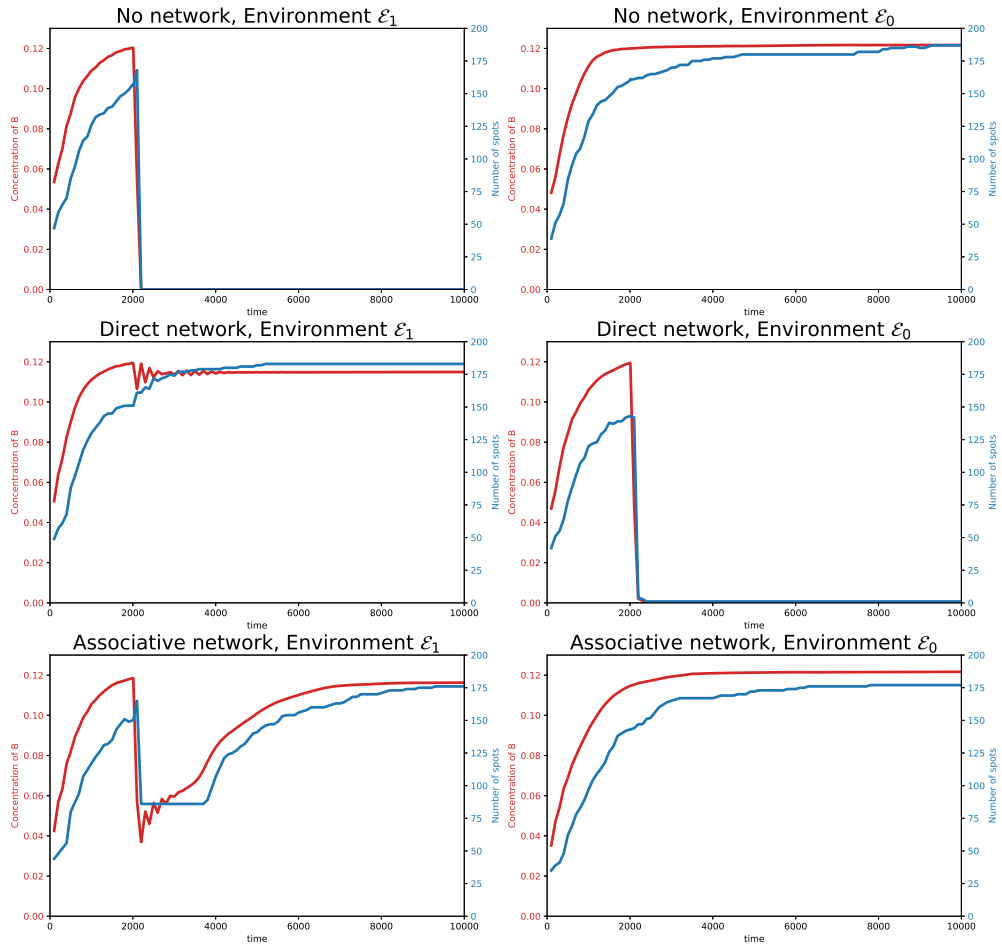


Figure 4: Time series of the average concentration of B and the number of $GS\Sigma$ s in the case of uniform bolus delivery, for the two environments and the three networks considered. Left column: environment \mathcal{E}_1 , right column: environment \mathcal{E}_0 , top: no network, middle: direct network \mathcal{N}_D with $k_D = 0.06$, bottom: associative learning network \mathcal{N}_A with $k_L = 2.5 \times 10^{-4}$.

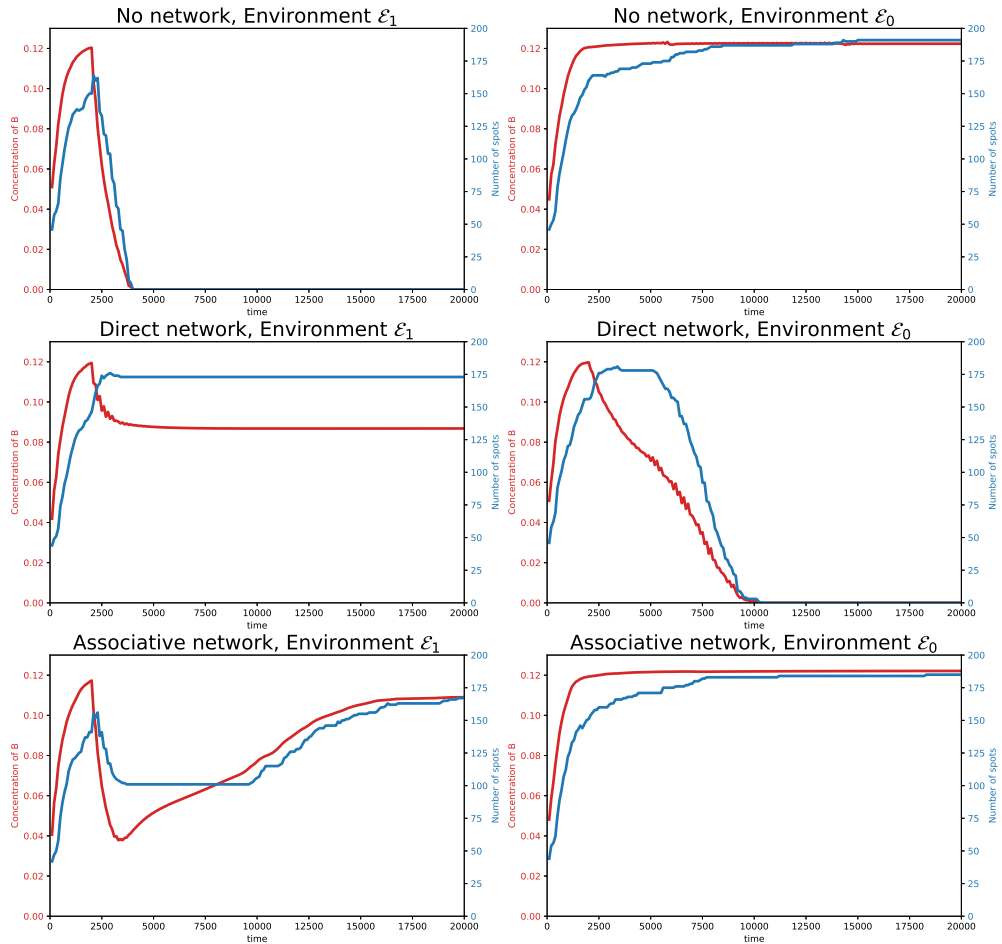


Figure 5: Time series of the average concentration of B and the number of spots in the case of boundary diffusion bolus delivery, for the two environments and the three networks considered. Left column: environment \mathcal{E}_1 , right column: environment \mathcal{E}_0 , top: no network, middle: direct network \mathcal{N}_D with $k_D = 0.0025$, bottom: associative learning network \mathcal{N}_A with $k_L = 7.5 \times 10^{-5}$.

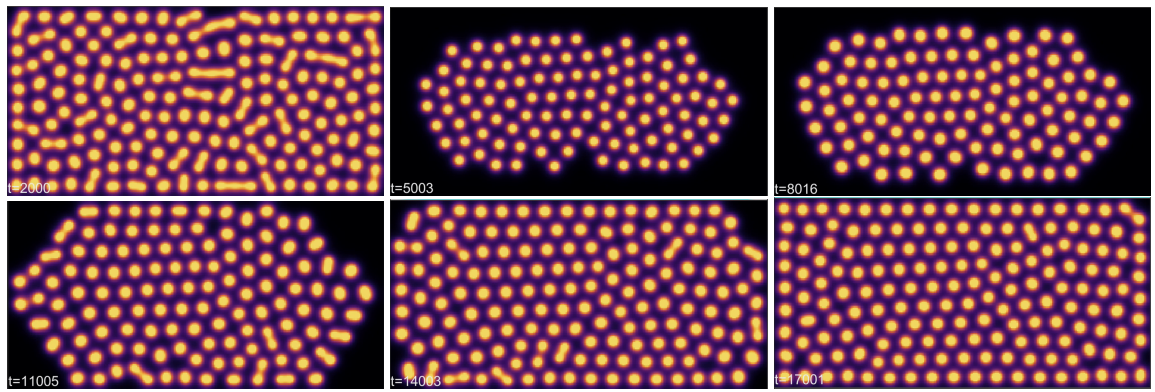


Figure 6: Snapshots of the Gray-Scott B component at regular time intervals in the boundary delivery case, for the associative learning network \mathcal{N}_A placed in \mathcal{E}_1 . This sequence corresponds to the bottom left panel of Figure 5.